

The N-Body Problem: Parallel Execution from Single-Person Egocentric Video

Zhifan Zhu¹* Yifei Huang² Yoichi Sato² Dima Damen¹

¹University of Bristol, United Kingdom ²The University of Tokyo, Japan

<https://zhifanzhu.github.io/ego-nbody>

Abstract

Humans can intuitively parallelise complex activities, but can a model learn this from observing a single person? Given one egocentric video, we introduce the N-Body Problem: how N individuals, can hypothetically perform the same set of tasks observed in this video. The goal is to maximise speed-up, but naive assignment of video segments to individuals often violates real-world constraints, leading to physically impossible scenarios like two people using the same object or occupying the same space. To address this, we formalise the N-Body Problem and propose a suite of metrics to evaluate both performance (speed-up, task coverage) and feasibility (spatial collisions, object conflicts and causal constraints). We then introduce a structured prompting strategy that guides a Vision-Language Model (VLM) to reason about the 3D environment, object usage, and temporal dependencies to produce a viable parallel execution. On 100 videos from EPIC-Kitchens and HD-EPIC, our method for $N = 2$ boosts action coverage by 45% over a baseline prompt for Gemini 2.5 Pro, while simultaneously slashing collision rates, object and causal conflicts by 55%, 45% and 55% respectively.

1. Introduction

As humans, we can naturally decide when and where to split tasks to complete them faster, without disrupting the flow of others. This suggests that even tasks performed by a single person contain hidden opportunities for parallelisation. In unscripted egocentric videos, prior works have shown that the camera wearer often carries out multiple goals in parallel [22, 26, 28, 29]. This raises an intriguing question: can we predict a parallel execution of multiple agents, such that the original work can be sped up?

We introduce and formalise **the N-Body Problem** – the novel problem of predicting a multi-agent parallel execu-

tion from a video showcasing a single-agent execution trace. Our output should imagine a highly synergetic execution which maximises the concurrent work performed by all agents. This effective execution is not merely an optimisation problem for speed. It is fundamentally constrained by the physics and logic of the real world. Any valid parallel execution must respect several categories of constraints: First, the *Spatial Constraints*. As physical entities, the N agents cannot occupy the same space simultaneously. The execution must therefore aim to be collision-free. Second, the *Object Constraints*. The execution must enforce exclusive object ownership, ensuring that no two agents attempt to use the same object at the same time. Finally, the *Causality Constraints*. To be causally correct, the execution must respect when certain actions are prerequisites for others.

It might be tempting to think of the N-Body Problem as a resource-constrained scheduling task. We argue this is infeasible for long-form, unscripted video. A 25-minute video comprises hundreds of thousands of frames, and no existing model can robustly parse this continuous stream into a scheduling task. Similarly, it is infeasible to produce a robust discrete, hierarchical task graph as explored in prior work [1, 9, 20]. These works are restricted to shorter videos where one is carrying out a known pre-defined activity. This is not the case in unscripted videos where multiple ongoing goals [26] are carried out. We instead consider the N-Body Problem a joint reasoning and temporal segmentation problem that requires a holistic understanding of what to do, where, with what, and in what order, all at once.

We evaluate the N-Body Problem on 100 long videos from single-person egocentric datasets [4, 24] (avg 25min). We propose a suite of metrics that leverage existing ground-truth annotations (actions, object tracks, camera poses) to evaluate a plan’s performance (Goals) and, critically, its physical feasibility (Constraints). Crucially, this ground truth is not used as input, but only to evaluate the feasibility of proposed executions. We argue that defining a single “ground-truth” execution is an ill-defined and infeasible task. For any complex activity, there exist multiple valid and

*Partly conducted during Z Zhu’s visit to the University of Tokyo.

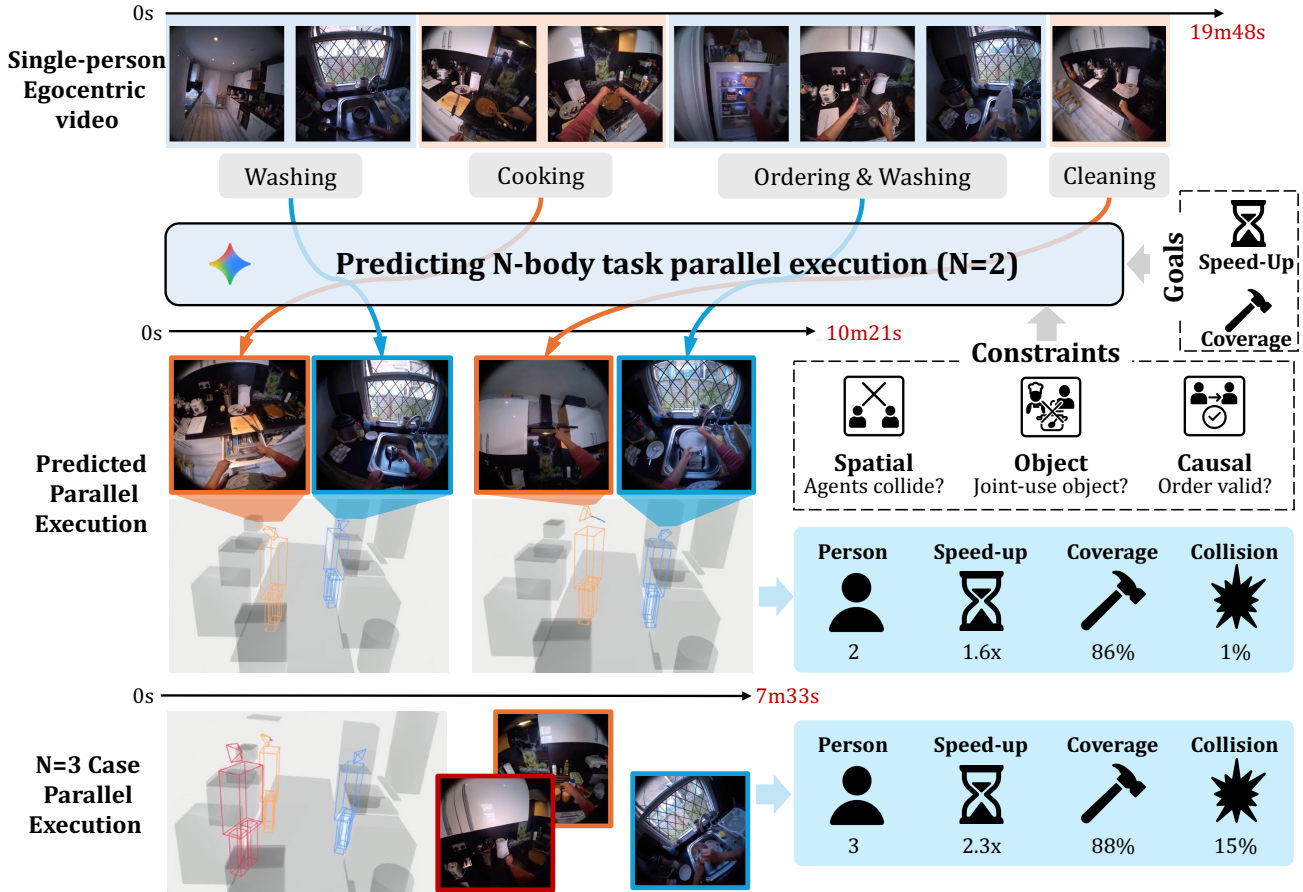


Figure 1. **Top.** Our input is single-person egocentric video. The camera wearer performs a combination of cooking, washing up and ordering. **Middle.** Predicted 2-Body Parallel execution. Our method, which uses Gemini with prompts on goals and constraints, achieves a 1.6x speed-up (from 19.8min to 10.4min) with 86% coverage. We show 3D representation of where the 2-agents (orange/blue) are and their camera views. P1 is mostly left to do the cooking, while P2 is washing up and ordering. **Bottom.** 3-Body parallel execution achieving further 2.3x speed-up to 7.5min. P2 is washing up while P3 is drying and storing things away. For the full output, see supp and supp video.

(near-)optimal parallel solutions. Therefore, our framework evaluates any generated plan based on its intrinsic properties and adherence to real-world feasibility, rather than comparison to a single arbitrary reference.

To establish a benchmark and analyse the challenges of this problem, we leverage a state-of-the-art VLM, Gemini 2.5 Pro [3]. This VLM has produced outstanding performance on a number of long-form video tasks [3, 24]. We design a structured prompting strategy that guides the VLM to reason about 3D environments, object usage, and task dependencies. This approach allows the VLM to better capture the constraints for a viable parallel execution. While we do not contribute to a better video understanding/reasoning model, using our proposed metrics, we systematically analyse the VLM’s performance and demonstrate how it can be controlled to trade off between goals and constraints. Fig 1 shows an output of our method, where we predict a 2-Body and 3-Body executions from the same video.

To summarise, in this paper we:

- Formulate the N-Body Problem – parallelising a multi-agent execution from a single-agent trace.
- Propose an evaluation metrics suite of parallel execution using publicly available annotations.
- Design a complex prompt that allows state-of-the-art VLM to act as a reasoning model, to solve the N-Body Problem, maximising goals and respecting spatial, object and causal constraints.
- Evaluate on 100 long videos from two single-person datasets [4, 24] for both 2-Body (N=2) and 3-Body (N=3) execution.
- Demonstrate the difficulty of this problem, where naive assignment and optimisation scheduling produce significant collision rate (25.9% and 39.7%) between agents, and open-weight VLM QWEN fails to speed-up. While Gemini 2.5 Pro with base prompt performs poorly, it can be guided to improve goals and respect constraints, im-

proving action coverage to 91.3% and reducing collision, object and causal conflict – to 7.7%, 0.64% and 18% on 80 HD-EPIC videos, respectively.

2. Related Works

Egocentric Videos. Popularised by recent datasets [4, 8, 9, 13, 24], egocentric vision has produced powerful models for parsing human activity streams. Current research spans action understanding [7, 12, 25], multimodal sensing [11, 17, 40], and vision-language tasks [16, 18, 37, 41]. While this paradigm excels at passive understanding along one timeline, it does not address the challenge we study: how to re-allocate the same work across multiple concurrent workers while remaining faithful to real-world feasibility (space, objects and semantics). Task-graph annotation [9, 20] is a promising bridge for enforcing causal order. However, these annotations are not publicly available, limiting comprehensive multi-constraint evaluation. We here focus on predicting parallel execution with goals and constraints that leverage readily available signals.

Task Parallelisation. Prior works on multitasking and coordination shows that human activity often interleaves goals and that latent “threads” can be unwoven from a single stream, revealing headroom for concurrency [26, 29]. Multi-person egocentric and mixed-view collections further indicate that collaborative behaviours are learnable in principle [14, 15, 27, 38]. However, prior works focus only on describing or segmenting concurrent intentions. [14] is the closest work to our paper, as the Lemma dataset records one person performing the task, then records two people collaborating to complete the same task without verbal communication. While the intuition matches others, the videos are short-term (only 2 mins). Additionally, none of the works above predicts a parallel execution from a single demonstration. At the abstract level, our problem is analogous to task scheduling in parallel computing [5, 31]: given a set of dependent tasks and limited processors, the goal is to minimise the *makespan*. Since optimal scheduling is challenging, practical solutions rely on heuristics (*e.g.* list scheduling such as HEFT) that deliver approximations efficiently [33]. We include a HEFT-style baseline in our results.

Spatial Reasoning in Vision-Language Models. While Vision-Language Models (VLMs) have demonstrated impressive capabilities, recent work has consistently shown that spatial reasoning remains a significant weakness [10, 32, 35]. This limitation is often attributed to the lack of explicit 3D and geometric information in pre-training. Current research aims to mitigate this through methods like fine-tuning on synthetic 3D VQA datasets [19, 23, 39] or developing specialized architectures [2, 21, 30]. We address this limitation from a task-driven angle. Rather than pursuing a universally capable spatial reasoner, we ask how to elicit

reliable spatial behaviour for our downstream goal: collision avoidance in predicting parallel execution. Our spatial prompt discretises the environment and breaks the temporal timeline into zone-aligned periods in order to guide the spatial reasoning in the VLM without changing model weights.

3. Problem Formulation

While the general gist of acquiring help from others during everyday operation is intuitive, formulating the problem as a representation mapping from one video to N parallel executions needs significant attention. We introduce the input and output for the N-Body Problem in Sec 3.1. We then separate the objectives into goals (Sec 3.2) and constraints (Sec 3.3). These identify what needs to be maximised, versus what makes a parallel execution incorrect or invalid.

3.1. Input and Output Representations

We denote the source input video as \mathcal{I} , which represents a single-person execution from frame 1 to $T_{\mathcal{I}}$. The problem is to divide \mathcal{I} into non-overlapping assignable segments,

$$S_{ij} = [\mathcal{I}_i, \mathcal{I}_j], \quad i < j; \quad \forall ij, i'j' \rightarrow IoU(S_{ij}, S_{i'j'}) = 0. \quad (1)$$

It is critical that these segments are non-overlapping so they can be assigned to a single agent in the N-Body Problem. Note that some parts of the original video \mathcal{I} might not be assigned to any segment S_{ij} and are accordingly discarded.

For an N -Way parallel execution $\mathcal{P} = \{\mathcal{P}_1, \mathcal{P}_2, \dots, \mathcal{P}_N\}$, we then need to assign each of these executable segments to one of the N agents. Importantly, the order of the segments can be shuffled if needed. Additionally, any agent can be in an idle state as they wait for a viable task to perform. Denote \mathcal{P}_n the execution assigned to the n -th agent, and denote $\mathcal{A}(\cdot, \cdot)$ the assignment function,

$$\mathcal{A}(S_{ij}, \mathcal{P}_n) = \tau \quad (2)$$

means that the start of the segment S_{ij} is assigned to the frame τ in \mathcal{P}_n . As the duration of that segment remains unchanged, the task is only to assign a start time for that segment at \mathcal{P}_n . Consequentially, the frames $[\tau, \tau + |S_{ij}|]$ in the parallel execution \mathcal{P}_n are all allocated to the segment:

$$\mathcal{A}(S_{ij}, \mathcal{P}_n) = \tau \rightarrow \mathcal{P}_n[\tau, \tau + (j - i)] = S_{ij} \quad (3)$$

Additionally, a segment can only be assigned to a single agent, *i.e.*

$$\mathcal{A}(S_{ij}, \mathcal{P}_n) \neq null \rightarrow \forall m \neq n : \mathcal{A}(S_{ij}, \mathcal{P}_m) = null, \quad (4)$$

where $\mathcal{A}(S_{ij}, \mathcal{P}_n) \neq null$ indicates that the segment S_{ij} is assigned to \mathcal{P}_n at some frame.

Of course there are many possible ways to divide segments and also many ways to assign these segments to

agents, leading to different parallel executions $\{\mathcal{P}\}$ from the same video \mathcal{I} . We next define the one(s) we are after in the N-Body Problem.

3.2. Goals

Our objective is to generate one parallel execution \mathcal{P} that is as efficient as possible while covering as much of the work completed in the source execution \mathcal{I} as possible. Formally, we aim to maximise the following quantities:

First, the coverage of the parallel execution:

$$\text{Coverage} := \frac{\text{Number of assigned frames}}{T_{\mathcal{I}}} \quad (5)$$

where we calculate the total length of all assigned – hence covered – segments in the original video.

Second, the speed-up from the original video to parallel execution:

$$\text{Speed-Up} := \frac{\text{Sequential execution time}}{\text{Parallel execution time } (T_{\mathcal{P}})}, \quad (6)$$

where $T_{\mathcal{P}}$ amounts to the time required for the agent that is working the longest.

3.3. Constraints

While maximising the above objectives, the generated execution must also remain physically and logically feasible. We therefore seek to measure from only the given video, and avoid (i.e. minimise) violations of four constraints – the first two are related to the space in the scene and the second two are the semantics of objects and causal actions.

First, the collision in the 3D scene between concurrent working agents. Agents should not be occupying the same space at one time. We measure conflicts in the space through the collision rate:

$$\text{Collision Rate} := \frac{\text{Number of colliding frames in } \mathcal{P}}{T_{\mathcal{P}}}, \quad (7)$$

Second, the relocation overhead – i.e. “jump” distances of agents in the parallel execution. As each agent n is assigned different segments, at times the end of one segment can be at a different part of the scene than the start of the next segment. This is a violation as it expects the agent to unrealistically *teleport* in space. We measure this jump conflict as:

$$\text{Spatial Jump} := \frac{1}{N} \sum_{n=1}^N \text{Avg. Jump Distance of agent } n, \quad (8)$$

Third, the conflict of accessing the same object by different agents. Denote \mathcal{O} the set of objects accessed or used in the video. A conflict is measured as the duration when multiple agents access the same object $\mathcal{O}_k \in \mathcal{O}$ in the parallel

execution. The object conflict rate (OCR) is defined as:

$$\text{OCR} := \frac{\text{Num. of frames where } \exists \mathcal{O}_k \in \mathcal{O} \text{ in conflict}}{T_{\mathcal{P}}}, \quad (9)$$

Note that we here make the assumption that no extra objects in the scene can be used instead - e.g. if two knives are used during the activity, we assume these are the only knives available. Given we only rely on the observations from a single video, it will be challenging to make assumptions about additional objects or their utility – e.g. a suitable alternative knife for slicing bread.

Lastly, a causal constraint is one that measures plausible parallel executions – i.e. preserve any tasks that need to occur in a particular order or need to take a specific time to complete. For example, an agent needs to first chop the vegetables before adding these to the soup – this order should not be reversed in the parallel execution. We measure causality violations rate (CVR) as:

$$\text{CVR} := \frac{\text{Num. of violated } \mathcal{G}_k \in \mathcal{G}}{|\mathcal{G}|} \quad (10)$$

where \mathcal{G} is the list of causal constraints. Each constraint in \mathcal{G} is a pair of temporal segments that must occur in order. If any segment pair is reversed, carried out in parallel or the prerequisite segment is missing, i.e., missing the cause, the pair \mathcal{G}_k is considered a causality violation. We calculate the rate of violated pairs amongst all causal pairs. Note that if all pairs are ordered correctly, the complete causal graph is thus correctly executed.

Objectives Summary. We have defined multiple objectives for the N-Body Problem, as no single measure can capture the quality of a parallel execution on its own. The distinction between goals and constraints is not absolute: for example, coverage could be treated as a constraint, while jump distance could also be viewed as a goal. In this work, we treat goals as objectives to maximise and constraints as objectives to avoid or minimise. The precise implementation of goals and constraints as quantitative metrics is in Sec 4.2. Importantly, multiple parallel executions $\{\mathcal{P}\}$ can achieve the same performance (speed-up, coverage, collision/conflict/causality rates). We consider these to be *equivalent*.

4. Experiments

4.1. Datasets and Annotations

We evaluate our formulation on two egocentric datasets: HD-EPIC [24] and EPIC-KITCHENS-100 (which we refer to as EPIC in the rest of the paper) [4]. Both capture unscripted kitchen-based activities in home environments, with long continuous recordings that naturally contain interleaved goals such as cooking, cleaning, and storing. We randomly select 100 long videos – 80 from HD-EPIC and 20 from EPIC, covering 24 unique scenes (9 from HD-EPIC

and 15 from EPIC) – with minimum duration of 10 minutes (avg video length 25.3 minutes) to form a tractable evaluation set. The longer videos are likely to be more meaningful for parallel execution as they tend to capture more underlying activities. Crucially, both datasets provide ground-truth annotations to evaluate the goals and constraints (presented in Sec 3) using a set of dedicated metrics (see Sec 4.2). We select more videos from HD-EPIC as they contain additional ground truth that helps us evaluate object and causal conflict as we will describe below.

Ground-Truth Camera Poses. Both HD-EPIC and EPIC provide ground-truth camera poses annotated using multi-sensor SLAM [6] or sub-sampled frames COLMAP [34]. Camera poses provide strong signal of where the person situates in the environment, as well as their body orientations. With the person’s trajectory given by the camera poses in the source video, we are able to evaluate the Collision Rate.

Ground-Truth Actions. Both HD-EPIC and EPIC provide dense and detailed annotations of all action segments completed by the camera wearer. The action narrations covers all meaningful parts of the video, which we will use for measuring the coverage of important works in the original video.

Ground-Truth Object Movements. Recently introduced HD-EPIC provides extensive manual annotations of object movements as object tracks. These are start-end segments that correspond to the duration when an object is moved by the camera-wearer along the video. These are exhaustive and form long trajectories covering frames when the object is in motion/use versus when the object is stationary. These tracks are linked to the object instances, allowing us to identify the same instance of any object throughout the video. The presence of these annotations allow us to accurately measure object conflict.

Ground-Truth Recipe Segments Dependencies. Similarly, the recently introduced HD-EPIC dataset contains annotated time segments of recipe preparation and recipe steps. For each recipe, the steps are manually defined along with labels for the temporal segments for each step. Additionally, any preparatory action is also manually labelled (e.g. for the step of ‘boiling pasta’, the prep of ‘filling the kettle with water’ is temporally segmented and linked to this step). Additionally, we add strict dependencies between steps of one recipe manually (see Supp for details). These annotations allow us to evaluate the following causal constraints in the parallel execution: i) prep-step constraint: a prep must be completed before the corresponding step starts, and ii) step-step constraint: for the step dependency ($A \rightarrow B$), the step A must be finished before B starts.

4.2. Evaluation Metrics

As noted in the introduction, we do not have any ground truth parallel executions – i.e. we only have access to single-

person video inputs. Importantly, such ground truth cannot be acquired even if two people are hired to carry out the same task, as this will only provide one of many possible valid parallel executions. Instead, we rely on identifying invalid executions through our proposed evaluation metrics.

Our evaluation metrics directly measure the goals (Sec. 3.2) and constraints (Sec. 3.3), using the available data annotations, as follows: frame coverage \uparrow , action coverage \uparrow , speed-up \uparrow , 3D spatial collision rate \downarrow , object conflict rate (OCR) \downarrow , average jump distance \downarrow and causality violation rate (CVR) \downarrow .

The frame coverage of the parallel execution is implemented as in Equation (5):

$$\text{Frame Coverage} := \frac{\sum |S_{ij}| \iff \exists n; \mathcal{A}(S_{ij}, \mathcal{P}_n) \neq null}{T_{\mathcal{I}}}, \quad (11)$$

where $\mathcal{A}(S_{ij}, \mathcal{P}_n) \neq null$ means the segment S_{ij} is assigned to the agent n in the parallel execution \mathcal{P} . Note again that one segment can only be assigned to a single agent.

While frame coverage is one way to measure parallel execution, some frames might be excluded that do not correspond to any tasks or actions. Instead, we use the exhaustive annotations for action segments, we consider the set of all actions in the video \mathcal{C} and compute the percentage of these actions that are covered by the parallel execution. We calculate the action coverage as:

$$\text{Action Coverage} = \frac{\sum_{\mathcal{C}_r \in \mathcal{C}} \mathbb{1}[\exists n, i, j: \mathcal{A}(S_{ij}, \mathcal{P}_n) \neq null \ \& \ IOU(S_{ij}, \mathcal{C}_r) \geq 0.5]}{|\mathcal{C}|}, \quad (12)$$

i.e. we calculate the temporal overlap between the action segment \mathcal{C}_r and any assigned segments in the parallel execution \mathcal{P}_n . As long as any agent n has a segment that temporally overlaps with the action by more than 0.5 IOU, we consider the action to be covered by this parallel execution. We use the standard threshold of temporal overlap (0.5) which is accepted in temporal action localisation. Note that this strict threshold 0.5 implies that the action cannot be covered by multiple agents as any other agent will naturally have a threshold lower than 0.5 IOU.

To disentangle the coverage from the speed-up, we calculate the speed-up metric as:

$$\text{Speed-Up} = \frac{\sum_{t=1}^{T_{\mathcal{I}}} \mathbb{1}[\exists n, i, j: \mathcal{A}(S_{ij}, \mathcal{P}_n) \neq null \ \& \ i \leq t \leq j]}{T_{\mathcal{P}}}. \quad (13)$$

Note that the speed-up metric does not account for the frames that are *not* covered by the parallel execution \mathcal{P} . It measures the relative speed-up from sequential execution to parallel execution solely. We disentangle the two metrics (coverage and speed-up) to avoid solutions that drop the coverage to gain speed-up.

To evaluate the spatial collision between parallel agents, we use the ground-truth camera poses to represent person’s

trajectory. Denote $\Gamma_n(t)$ the spatial trajectory of the n -th agent at frame t , the collision rate is implemented as:

$$\text{Collision Rate} = \frac{\sum_{t=1}^{T_{\mathcal{P}}} \mathbb{1}[\exists n \neq n' : is_collide(\Gamma_n(t), \Gamma_{n'}(t))]}{T_{\mathcal{P}}}, \quad (14)$$

where $is_collide(\cdot, \cdot)$ is a function that determines whether two different agents occupy the same space, based on their body positions and orientations in the world coordinate system; the $is_collide(\cdot, \cdot)$ function is implemented using the average of size of human body¹.

The jump distance is implemented as:

$$\text{Jump} = \frac{1}{N} \sum_{n=1}^N \frac{1}{M_n} \sum_{m=1}^{M_n-1} \|\Gamma_n(start_{m+1}) - \Gamma_n(end_m)\|, \quad (15)$$

where M_n is the total number of segments assigned to the n -th agent, $start_{m+1}$ is the start frame of the segment $m+1$ and end_m is the end frame of the segment m .

To quantify object conflict, we use the object movement tracks. Denote \mathcal{O} the set of objects accessed, moved or used in the source video. A single object conflict is the duration when multiple agents move the same object $\mathcal{O}_k \in \mathcal{O}$ in the parallel execution. The object conflict rate (OCR) can thus be implemented as:

$$\text{OCR} = \frac{\sum_{t=1}^{T_{\mathcal{P}}} \mathbb{1}[\exists \mathcal{O}_k \in \mathcal{O}, \exists n \neq n' : \mathcal{O}_{k,n}(t) \wedge \mathcal{O}_{k,n'}(t)]}{T_{\mathcal{P}}}, \quad (16)$$

where $\mathcal{O}_{k,n}$ is 1 if the object \mathcal{O}_k is accessed by agent n at frame t , and 0 otherwise.

Importantly, to quantify the violation of causality, we use the ground-truth available in the dataset that identifies the dependencies between preparatory actions (e.g. ‘get knife’) and step actions (‘cut vegetable’) within a recipe, as well as causal dependences amongst steps of the same recipe. Denote \mathcal{G} the set of segment pairs, $\mathcal{G} = \{(\mathcal{G}_{\ell,0} \rightarrow \mathcal{G}_{\ell,1})\}$ where the action $\mathcal{G}_{\ell,1}$ depends on the finishing of the prerequisite $\mathcal{G}_{\ell,0}$. The causality violation rate (CVR) is implemented as:

$$\text{CVR} = \frac{\sum_{(\mathcal{G}_{\ell,0} \rightarrow \mathcal{G}_{\ell,1}) \in \mathcal{G}} \mathbb{1}[\exists n, n' : E(\mathcal{G}_{\ell,0}, \mathcal{P}_n) > S(\mathcal{G}_{\ell,1}, \mathcal{P}_{n'})]}{|\mathcal{G}|}, \quad (17)$$

where $E(\mathcal{G}_{\ell,0}, \mathcal{P}_n)$ is the end time of the segment in \mathcal{P} and $S(\mathcal{G}_{\ell,1}, \mathcal{P}_{n'})$ the start of $\mathcal{G}_{\ell,1}$ in any agent \mathcal{P} ’s execution. Note that CVR also evaluates any causal constraint violation within one agent’s execution when $n \equiv n'$.

4.3. Model Setup

We use Gemini 2.5 Pro [3] to generate parallel execution \mathcal{P} from input video \mathcal{I} . The input to the Gemini model are formed by two parts: our proposed text prompt and the video input \mathcal{I} . We use the default 1FPS frame sampling rate to fit the maximum context.

¹46 cm wide and 25 cm deep

We progressively evolve more specific system prompts to improve Gemini 2.5 Pro’s performance on the N-Body Problem:

- **Base Prompt.** The basic prompt where we simply inform the model about the task, without mentioning any goals and constraints.
- **+ Goals-Only.** On top of “Base”, we instruct the model to maximise the goals (Coverage and Speed-Up), without mentioning any constraints.
- **+ Goals-and-Constraints.** We instruct the model to both maximise the goals (Coverage and Speed-Up) and minimise the constraints of space, object and semantics.
- **+ Spatial Prompt.** On top of “+ Goals-and-Constraints”, we provide an *additional* column-separated-value (csv) file linking spatial location to time—temporal durations in the source video. We instruct the model to avoid occupying the same zone for different agents.

Regarding the final “+ Spatial Prompt”, current vision-language models – including Gemini 2.5 Pro – often struggle with robust spatial understanding. In the parallel-execution problem, simply supplying the raw trajectory of the source video as additional input does not provide Gemini with sufficient guidance (see ablation in supplementary). We explore a compact and structured spatial prompt that explicitly encodes the knowledge needed for collision avoidance. We divide the 3D environment into equal-sized zones; we divide the XY-plane as the majority of movements happen within the ground plane. We then extract the duration when the person in \mathcal{I} remains within one zone, producing a list of triplets of: (start-time, end-time, zone number). We then instruct Gemini 2.5 Pro to avoid assigning two parallel agents working in the same zone concurrently.

The complete prompt can be found in the supplementary. We set Gemini parameter temperature= 0 and top_p = 0.2 for more deterministic results.

Additional Comparison Methods. In addition to Gemini 2.5 Pro, we evaluate an open-weight model Qwen2.5-VL-72B [36] under our full prompt and 1 FPS sampling rate. We introduce a naive baseline that divides the video into equal halves and has the two agents execute their halves concurrently, without modelling dependencies. Additionally, we evaluate a simple HEFT-style list scheduler [33]. For the scheduler, we turn ground-truth action timestamps into assignable segments, using the privileged knowledge of start-end times of actions, and manually induce simple precedences from verb-object cues (e.g. *take* → *use* → *put*, *open* → *close*). We then apply a standard list scheduling heuristic: at each step, select the first ready task and place it at the earliest feasible time that respects object exclusivity. We further experiment removing the ground-truth action timestamps signal: we divide the input duration into 1-minute windows and concatenate all action narrations appearing within each 1-min. We then use the same heuris-

Method		Coverage (%) [†]	Action Cov. (%) [†]	Speed-Up [†]	Coll. Rate (%) [↓]	Jump (m) [↓]	OCR (%) [↓]	CVR (%) [↓]
2-Body Problem	Naive Half-Half	<u>100.0</u>	<u>100.0</u>	<u>2.00</u>	25.9	<u>0.00</u>	3.61	<u>14.7</u>
	HEFT 1-min	99.9	100.0	1.93	39.7	0.65	2.53	16.7
	HEFT GT start-end [†]	77.6	99.2	1.82	59.1	0.28	0.03	72.5
	Qwen2.5-VL-72B*	63.9	63.4	0.89	<u>0.2</u>	0.19	<u>0.00</u>	45.2
	Gemini2.5 (Base Prompt)	61.4	62.9	1.58	17.2	0.53	1.17	40.6
	+ Goals-Only	88.8	89.1	1.61	18.9	0.54	1.71	18.3
	+ Goals-and-Constraints	87.4	88.1	1.59	17.5	0.47	0.93	26.3
+ Spatial Prompt (ours)	90.7	91.3	1.40	7.7	0.55	0.64	18.0	
3-Body Problem (ours)		85.9	87.0	1.51	11.9	0.56	1.12	26.1

Table 1. Results on HD-EPIC. Notice that **bold** is across the various prompts of Gemini2.5. Underline implies best metric per column. *Qwen2.5-VL-72B could only generate results on a subset of 51/80 videos and fails for the rest. [†] uses action segment *ground-truth*. Causality Violation Rate (CVR) is evaluated on 60 videos that have recipe step annotations.

Method		Coverage (%) [†]	Action Cov. (%) [†]	Speed -Up [†]	Coll. Rate (%) [↓]	Jump (m) [↓]
2-Body Problem	Naive Half-Half	<u>100.0</u>	<u>100.0</u>	<u>2.00</u>	29.1	<u>0.00</u>
	HEFT 1-min	99.5	100.0	1.96	44.2	0.63
	HEFT GT start-end [†]	73.9	98.5	1.70	40.1	0.36
	Qwen2.5-VL-72B*	41.0	37.8	0.89	<u>0.3</u>	0.12
	Gemini2.5 (Base Prompt)	55.2	55.3	1.52	22.3	0.52
	+ Goals-Only	75.8	76.9	1.54	18.8	0.44
	+ Goals-and-Constraints	80.1	80.0	1.57	21.3	0.37
+ Spatial Prompt (ours)	89.9	90.6	1.35	10.1	0.43	
3-Body Problem (ours)		83.0	84.9	1.64	18.2	0.51

Table 2. Results on EPIC. Notice that **bold** is across the various prompts of Gemini2.5. Underline implies best metric per column. *Qwen2.5-VL-72B could only generate results on a subset of 7/20 videos. [†] uses *ground-truth* action segments.

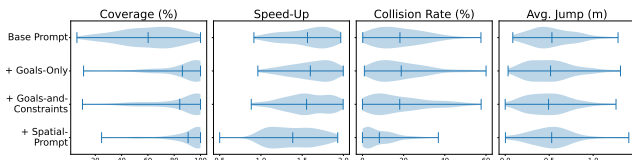


Figure 2. Distribution of evaluation metrics across all 100 videos as Gemini2.5 prompt is elaborated.

tics of verb-object cues to establish precedences in assigning these 1-min segments to agents.

4.4. Main Results

Table 1 shows the method performances on HD-EPIC. For each metric, we report the average metric over videos. Our prime set of comparative results are for $N = 2$ (2-Body Problem). We first present the naive baseline where we just assign the first half of the video to $P1$ and the second to $P2$. Results show very high collision rate and high object collision.

Gemini 2.5 Pro with base prompt produces good speed-up (1.58x), but considerably under-covers in frames and actions (62.9% action coverage) and produces a high collision rate (17.2%) and very high causality violation rate CVR (40.6%). Encoding goals in the prompt (+ Goals-only) achieves the highest speed-up and improves coverage, decreasing causality violation rate (CVR) significantly. En-

coding constraints drops the speed-up but fails to reduce the spatial collision rate. Spatial prompting (**ours**) reduces the collision rate by a large margin, increases the coverage but has a slightly lower speed-up. Table 2 shows similar trend on EPIC evaluation videos.

While tables 1 and 2 only present averaged results across the videos, figure 2 shows the metrics distributions for Gemini2.5 as prompts is expanded. Introducing goals significantly improves the coverage. The spatial prompt consistently lowers the collision rate.

Both the naive baseline and HEFT scheduler produce significantly high collision rates, and removing the privileged ground-truth timestamps from HEFT produces a higher object conflict rate (OCR). Open-weight VLM Qwen2.5-VL-72B *fails to produce any output for 42 out of the 100 videos*. On the 58-video subset, it performs poorly in coverage even though it avoids collision – this model is incapable of solving this problem.

Table 1 and Table 2 also show the comparison results between 2-body and 3-body outputs. When scaling to 3-body, we observe a predictable increase in collision and object conflict rates (OCR), with better speed-up (1.40 \rightarrow 1.51 on HD-EPIC, vs 1.35 \rightarrow 1.64 on EPIC).

Qualitative samples are shown in Fig. 3 and best understood from the Supplementary video.

Result Analysis. To further understand how our method predicts parallel executions, we analyse three properties of the parallel execution across recipe-step annotated videos: cooking vs non-cooking task split, prep vs step split and differences in the walking distance. This analysis is presented in Figure 4.

First, we count the percentage of time an agent is carrying out cooking tasks (preps and steps for a recipe) vs non-cooking tasks (ordering or cleaning). We scatter-plot all videos (Figure 4 left) to compare the agent doing less cooking to one doing more cooking – (dots close to the axis $y = x$ correspond to a balanced split). Second, Figure 4 (middle) compares whether the prep for one step is performed by the same agent (self) or by the other agent. In most cases the prep is still carried out by the same agent per-

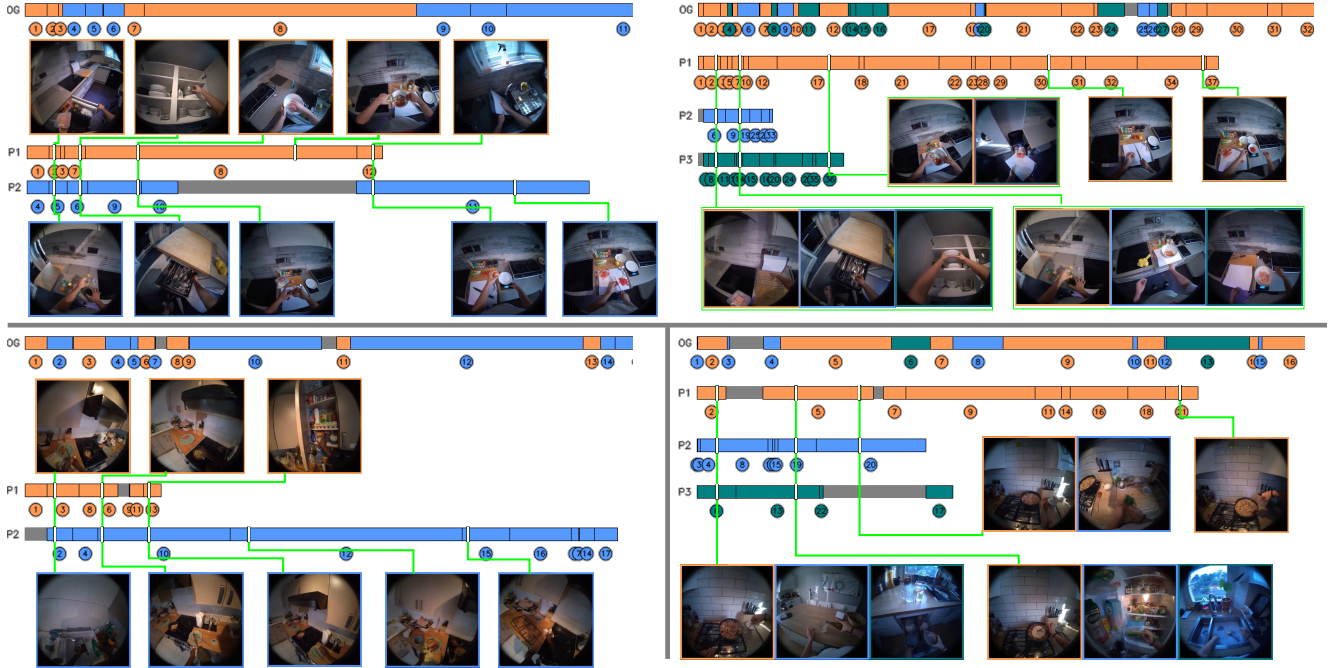


Figure 3. Qualitative results. **Top:** Same video with $N = 2$ and $N = 3$. Left: P1 is marinating chicken and washing up. P2 gathers spices (for the marination) in advance then prepares eggs. Right: P2 mostly fetches items from around the kitchen. **Bottom Left:** ($N = 2$) P2 is left to do the washing up and clearing. **Bottom Right:** ($N = 3$) P1 is cooking, P2 is pouring a glass of wine then puts stuff away. P3 is emptying the dishwasher then contributes to washing up.

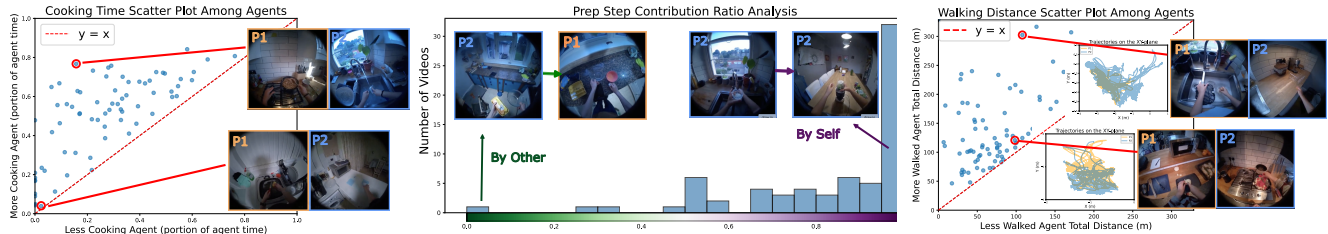


Figure 4. Analysis of parallel executions. **Left:** Distribution of agent cooking time (normalised by agent total time). *Top example:* P1 mostly cooks while P2 does the cleaning. *Bottom:* P1 and P2 both clean. **Middle:** The ratio of prep carried out by the same agent (Self) vs by the Other agent. *Left example:* P2 fetches the eggs and the bowl, P1 breaks the egg. *Right:* P2 fills the mixer cup and starts mixing. **Right:** Distribution of walking distances. *Top:* P1 is washing up while P2 moves around cleaning. *Bottom:* Both P1 and P2 walk equally.

forming the step. Third, we analyse the divide in the walking distance between agents. In most videos, one agent is doing significantly more walking than the other (dots much further than $y = x$). This supports the qualitative example in Fig. 3, and show this to be a common trend – one agent is left to occupy one hotspot while another agent moves around the space. We find this behaviour to be very natural and supports the validity of the parallel executions produced by the VLM using our proposed prompt.

5. Conclusion and Limitations

In this work, we introduce the N-Body Problem: predicting N-body parallel execution from a single egocentric video.

We design a structured prompt that guides a VLM to reason about the spatial, object and causal constraints, predicting the parallel execution, maximising goals while respecting constraints. Tested on 100 videos, our experiments show the difficulty of the N-Body Problem, and that Gemini 2.5 Pro can be guided by dedicated prompts to produce execution with high coverage and reasonable speed-up while maintaining low constraint violations.

While guided Gemini 2.5 Pro achieves remarkable results, we identify some of its limitations. For example, the model fails to maintain the exact time when needed – *e.g.*, the time where food should be boiling/brewing or in the microwave/oven is not maintained. Some task dependencies cannot be automatically discovered – *e.g.*, grinding coffee

beans is not automatically understood as a pre-requisite to brewing coffee. It also relies heavily on our explicit spatial prompt to avoid spatial collisions. These challenges suggest avenues for future research, to better model causality for unseen activities or develop architectures with more robust intrinsic spatial reasoning capabilities.

Acknowledgements Research at Bristol is supported by EPSRC UMPIRE EP/T004991/1, EPSRC PG Visual AI EP/T028572/1. Research at the University of Tokyo is supported by JST ASPIRE Grant Number JPMJAP2303, JSPS KAKENHI Grant Numbers JP24K02956 and 25K24384. Z Zhu is supported by UoB-CSC scholarship.

References

- [1] Kumar Ashutosh, Santhosh Kumar Ramakrishnan, Triantafyllos Afouras, and Kristen Grauman. Video-mined task graphs for keystep recognition in instructional videos. *Advances in Neural Information Processing Systems*, 2023. 1
- [2] Boyuan Chen, Zhuo Xu, Sean Kirmani, Brain Ichter, Dorsa Sadigh, Leonidas Guibas, and Fei Xia. SpatialVLM: Endowing vision-language models with spatial reasoning capabilities. In *Proceedings of the IEEE Conference on Computer Vision and Pattern Recognition*, 2024. 3
- [3] Gheorghe Comanici, Eric Bieber, Mike Schaekermann, Ice Pasapat, Noveen Sachdeva, Inderjit Dhillon, Marcel Blstein, Ori Ram, Dan Zhang, Evan Rosen, et al. Gemini 2.5: Pushing the frontier with advanced reasoning, multimodality, long context, and next generation agentic capabilities. *arXiv preprint arXiv:2507.06261*, 2025. 2, 6
- [4] Dima Damen, Hazel Doughty, Giovanni Maria Farinella, Antonino Furnari, Jian Ma, Evangelos Kazakos, Davide Moltisanti, Jonathan Munro, Toby Perrett, Will Price, and Michael Wray. Rescaling egocentric vision: Collection, pipeline and challenges for epic-kitchens-100. *International Journal of Computer Vision*, 2022. 1, 2, 3, 4
- [5] Pierre-François Dutot, Grégory Mounié, and Denis Trystram. Scheduling parallel tasks: Approximation algorithms. *Handbook of scheduling: Algorithms, models, and performance analysis*, 2004. 3
- [6] Jakob Engel, Kiran Somasundaram, Michael Goesele, Albert Sun, Alexander Gamino, Andrew Turner, Arjang Talattof, Arnie Yuan, Bilal Souti, Brighid Meredith, et al. Project aria: A new tool for egocentric multi-modal ai research. *arXiv preprint arXiv:2308.13561*, 2023. 5
- [7] Rohit Girdhar and Kristen Grauman. Anticipative video transformer. In *Proceedings of the IEEE International Conference on Computer Vision*, 2021. 3
- [8] Kristen Grauman, Andrew Westbury, Eugene Byrne, Zachary Chavis, Antonino Furnari, Rohit Girdhar, Jackson Hamburger, Hao Jiang, Miao Liu, Xingyu Liu, et al. Ego4d: Around the world in 3,000 hours of egocentric video. In *Proceedings of the IEEE Conference on Computer Vision and Pattern Recognition*, 2022. 3
- [9] Kristen Grauman, Andrew Westbury, Lorenzo Torresani, Kris Kitani, Jitendra Malik, Triantafyllos Afouras, Kumar Ashutosh, Vijay Baiyya, Siddhant Bansal, Bikram Boote, et al. Ego-exo4d: Understanding skilled human activity from first-and third-person perspectives. In *Proceedings of the IEEE Conference on Computer Vision and Pattern Recognition*, 2024. 1, 3
- [10] Yuping He, Yifei Huang, Guo Chen, Baoqi Pei, Jilan Xu, Tong Lu, and Jiangmiao Pang. EgoExoBench: A benchmark for first-and third-person view video understanding in mlms. *arXiv preprint arXiv:2507.18342*, 2025. 3
- [11] Yifei Huang, Minjie Cai, Zhenqiang Li, and Yoichi Sato. Predicting gaze in egocentric video by learning task-dependent attention transition. In *Proceedings of the European Conference on Computer Vision*, 2018. 3
- [12] Yifei Huang, Yusuke Sugano, and Yoichi Sato. Improving action segmentation via graph-based temporal reasoning. In *Proceedings of the IEEE Conference on Computer Vision and Pattern Recognition*, 2020. 3
- [13] Yifei Huang, Guo Chen, Jilan Xu, Mingfang Zhang, Lijin Yang, Baoqi Pei, Hongjie Zhang, Dong Lu, Yali Wang, Limin Wang, and Yu Qiao. EgoExoLearn: A dataset for bridging asynchronous ego- and exo-centric view of procedural activities in real world. In *Proceedings of the IEEE Conference on Computer Vision and Pattern Recognition*, 2024. 3
- [14] Baoxiong Jia, Yixin Chen, Siyuan Huang, Yixin Zhu, and Song-Chun Zhu. Lemma: A multi-view dataset for learning multi-agent multi-task activities. In *Proceedings of the European Conference on Computer Vision*. Springer, 2020. 3
- [15] Baoxiong Jia, Ting Lei, Song-Chun Zhu, and Siyuan Huang. EgoTaskQA: Understanding human tasks in egocentric videos. *Advances in Neural Information Processing Systems*, 2022. 3
- [16] Hyolim Kang, Yunsu Park, Youngbeom Yoo, Yeeun Choi, and Seon Joo Kim. Open-ended hierarchical streaming video understanding with vision language models. In *Proceedings of the IEEE/CVF International Conference on Computer Vision (ICCV)*, 2025. 3
- [17] Evangelos Kazakos, Arsha Nagrai, Andrew Zisserman, and Dima Damen. Epic-fusion: Audio-visual temporal binding for egocentric action recognition. In *Proceedings of the IEEE International Conference on Computer Vision*, 2019. 3
- [18] Kevin Qinghong Lin, Jinpeng Wang, Mattia Soldan, Michael Wray, Rui Yan, Zhongcong Xu, Difei Gao, Rong-Cheng Tu, Wenzhe Zhao, Weijie Kong, Chengfei Cai, WANG HongFa, Dima Damen, Bernard Ghanem, Wei Liu, and Mike Zheng Shou. Egocentric video-language pretraining. In *Advances in Neural Information Processing Systems*, 2022. 3
- [19] Dingning Liu, Cheng Wang, Peng Gao, Renrui Zhang, Xinzhu Ma, Yuan Meng, and Zhihui Wang. 3DAxisPrompt: Promoting the 3D grounding and reasoning in GPT-4o. *Neurocomputing*, 2025. 3
- [20] Weichao Mao, Ruta Desai, Michael Louis Iuzzolino, and Nitin Kamra. Action dynamics task graphs for learning plannable representations of procedural tasks. *arXiv preprint arXiv:2302.05330*, 2023. 1, 3
- [21] Damiano Marsili, Rohun Agrawal, Yisong Yue, and Georgios Gkioxari. Visual agentic AI for spatial reasoning with

- a dynamic api. In *Proceedings of the IEEE Conference on Computer Vision and Pattern Recognition*, 2025. 3
- [22] Stephen Monsell. Task switching. *Trends in cognitive sciences*, 7(3):134–140, 2003. 1
- [23] Michael Ogezi and Freda Shi. Spare: Enhancing spatial reasoning in vision-language models with synthetic data. *arXiv preprint arXiv:2504.20648*, 2025. 3
- [24] Toby Perrett, Ahmad Darkhalil, Saptarshi Sinha, Omar Emara, Sam Pollard, Kranti Parida, Kaiting Liu, Prajwal Gatti, Siddhant Bansal, Kevin Flanagan, Jacob Chalk, Zhifan Zhu, Rhodri Guerrier, Fahd Abdelazim, Bin Zhu, Davide Moltisanti, Michael Wray, Hazel Doughty, and Dima Damen. HD-EPIC: A Highly-Detailed Egocentric Video Dataset. In *Proceedings of the IEEE Conference on Computer Vision and Pattern Recognition*, 2025. 1, 2, 3, 4, 11
- [25] Chiara Plizzari, Shubham Goel, Toby Perrett, Jacob Chalk, Angjoo Kanazawa, and Dima Damen. Spatial cognition from egocentric video: Out of sight, not out of mind. In *2025 International Conference on 3D Vision (3DV)*, 2025. 3
- [26] Will Price, Carl Vondrick, and Dima Damen. Unweavenet: Unweaving activity stories. In *Proceedings of the IEEE/CVF conference on computer vision and pattern recognition*, 2022. 1, 3
- [27] Rachel Ringe, Mihai Pomarlan, Robert Porzel, and Rainer Malaka. Join me: Empirical means for gathering collaborative affordances. In *Mensch und Computer 2025-Workshopband*, 2025. 3
- [28] Joshua S Rubinstein, David E Meyer, and Jeffrey E Evans. Executive control of cognitive processes in task switching. *Journal of experimental psychology: human perception and performance*, 2001. 1
- [29] Yuhan Shen and Ehsan Elhamifar. Understanding multi-task activities from single-task videos. In *Proceedings of the IEEE Conference on Computer Vision and Pattern Recognition*, 2025. 1, 3
- [30] Chan Hee Song, Valts Blukis, Jonathan Tremblay, Stephen Tyree, Yu Su, and Stan Birchfield. Robospacial: Teaching spatial understanding to 2d and 3d vision-language models for robotics. In *Proceedings of the IEEE Conference on Computer Vision and Pattern Recognition*, 2025. 3
- [31] Roni Stern. Multi-agent path finding—an overview. *Artificial intelligence: 5th RAAI summer school*, 2019. 3
- [32] Ilias Stogiannidis, Steven McDonagh, and Sotirios A Tsafaris. Mind the gap: Benchmarking spatial reasoning in vision-language models. *arXiv preprint arXiv:2503.19707*, 2025. 3
- [33] Haluk Topcuoglu, Salim Hariri, and Min-You Wu. Performance-effective and low-complexity task scheduling for heterogeneous computing. *IEEE transactions on parallel and distributed systems*, 2002. 3, 6
- [34] Vadim Tschernezki, Ahmad Darkhalil, Zhifan Zhu, David Fouhey, Iro Laina, Diane Larlus, Dima Damen, and Andrea Vedaldi. Epic fields: Marrying 3d geometry and video understanding. *Advances in Neural Information Processing Systems*, 2023. 5
- [35] Jiayu Wang, Yifei Ming, Zhenmei Shi, Vibhav Vineet, Xin Wang, Sharon Li, and Neel Joshi. Is a picture worth a thousand words? delving into spatial reasoning for vision language models. *Advances in Neural Information Processing Systems*, 2024. 3
- [36] Peng Wang, Shuai Bai, Sinan Tan, Shijie Wang, Zhihao Fan, Jinze Bai, Keqin Chen, Xuejing Liu, Jialin Wang, Wenbin Ge, Yang Fan, Kai Dang, Mengfei Du, Xuancheng Ren, Rui Men, Dayiheng Liu, Chang Zhou, Jingren Zhou, and Junyang Lin. Qwen2-vl: Enhancing vision-language model’s perception of the world at any resolution. *arXiv preprint arXiv:2409.12191*, 2024. 6
- [37] Jilan Xu, Yifei Huang, Junlin Hou, Guo Chen, Yuejie Zhang, Rui Feng, and Weidi Xie. Retrieval-augmented egocentric video captioning. In *Proceedings of the IEEE Conference on Computer Vision and Pattern Recognition*, 2024. 3
- [38] Liang Xu, Chengqun Yang, Zili Lin, Fei Xu, Yifan Liu, Congsheng Xu, Yiyi Zhang, Jie Qin, Xingdong Sheng, Yunhui Liu, et al. Perceiving and acting in first-person: A dataset and benchmark for egocentric human-object-human interactions. *arXiv preprint arXiv:2508.04681*, 2025. 3
- [39] Jirong Zha, Yuxuan Fan, Xiao Yang, Chen Gao, and Xinlei Chen. How to enable LLM with 3D capacity? a survey of spatial reasoning in llm. *arXiv preprint arXiv:2504.05786*, 2025. 3
- [40] Mingfang Zhang, Yifei Huang, Ruicong Liu, and Yoichi Sato. Masked video and body-worn imu autoencoder for egocentric action recognition. In *Proceedings of the European Conference on Computer Vision*. Springer, 2024. 3
- [41] Sheng Zhou, Junbin Xiao, Qingyun Li, Yicong Li, Xun Yang, Dan Guo, Meng Wang, Tat-Seng Chua, and Angela Yao. Egotextvqa: Towards egocentric scene-text aware video question answering. In *Proceedings of the IEEE Conference on Computer Vision and Pattern Recognition*, 2025. 3

The N-Body Problem: Parallel Execution from Single-Person Egocentric Video

Supplementary Material

A. Additional Qualitative Figure and Videos

We show the expanded version of Fig. 1 in Figure 5. Here, we show the detailed split of the same video for $N = 2$ and $N = 3$ resulting in the speed-ups reported in Fig. 1, along with the 3D location of the agents over time and their relevant key-frames.

Additionally, we provide a diverse set of long clips from various videos of HD-EPIC and EPIC-Kitchens in our demonstration video (<https://youtu.be/06EbtEhHYPY>). For $N = 2$, we have 3 videos from HD-EPIC and 2 videos from EPIC-Kitchens. For $N = 3$, we have 2 videos from HD-EPIC and 1 video from EPIC-kitchens. Note that all the videos are played at $2\times$ speed to maintain a reasonable length (5min19s) for the demonstration video.

B. Spatial Prompt Variants

Above shown in Table 1 and Table 2 in the main paper, Gemini 2.5 Pro struggles with spatial collision of agents before introducing spatial prompt. In addition to the zone-related temporal segments introduced in 4.3, we experiment with different variants of providing spatial information to the VLM, specifically: (i) with raw trajectory, (ii) equal-sized zones with different sizes and (iii) using Gaussian Mixture Model (GMM) to cluster trajectory into zone with dynamic sizes. The proposed prompt uses zone size of 120x120cm.

Table 3 show comparison results of HD-EPIC. Raw trajectory reduces the collision rate by a small amount at the speed-up of $1.48\times$. However, GMM with 5 components and equal-sized zone of $40 \times 40\text{cm}$ achieve the same speed-up with much less collision rate. Increasing zone sizes leads to more reduced collision rates, but the speed-up increases accordingly, i.e. you are speeding-up less. With a larger zone size, the collision rate reduces more, but the speed-up also increases: an agent is unable to work when another agent owns a larger part of the space exclusively.

We show how different parameter and variants all contributes to the reduced collision rate, while trading-off speed-up differently, within and across grouping variant. HD-EPIC results in Fig. 8.

C. Recipe Causal Dependency Annotations

While HD-EPIC annotates the steps of the recipe, these steps are not necessarily causal and could occur in parallel. We thus annotate the step-step dependencies manually. We

study each recipe and identify steps which definitely need to occur in order. If there is doubt, we did not label the dependency as a causal one. For example, water needs to be boiled before being used for coffee brewing. From our 80 videos, we annotate 56 recipes, this results in 204 step-step segment dependencies. This corresponds to 60 videos, while the other 20 videos do not have recipes (i.e. are cleaning or ordering) or their recipes do not have step-step dependencies. In Figure 7, we showcase 4 examples of the annotated recipe step-step dependencies.

We additionally use the prep-step dependency provided by the HD-EPIC dataset [24], and there are 728 prep-step segment dependencies in above 60 videos. To see prep-step annotation samples, please refer to HD-EPIC [24].

Overall, the reported Causality Violation Rate (CVR) is evaluated on 932 causal constraints across 60 videos combining both prep-step and step-step annotations.

As there are two types of causal constraints in the annotation: prep-step and step-step (see Section 4.1 and Section C), we break down the Causal Violation Rate (CVR) according to the type of constraint violated. Furthermore, each violation error is classified into two categories: i) segment pair is reversed or ii) the cause is missing. We report these categories separately.

Table 4 shows the CVR results breakdown. Naive Half-Half and HEFT 1-min have lowest Miss errors by design, but have highest Reverse errors. On the other hand, HEFT GT start-end and Qwen2.5-VL-72B have lowest Reverse errors, but with high Miss errors. Relatively, Gemini 2.5 based methods are balanced in both Reverse and Miss. Among Gemini 2.5 based methods, "+ Goal-Only" achieves the lowest total causal error, and our spatial prompt maintains a comparable performance.

In Figure 6, we normalise both the Reverse Error and the Miss Error by their respective total counts, and present their distributions across videos. Evidently our proposed prompt (ours) achieves the lowest rate in reversal and missed rate. Increasing the number of agents $N = 3$ results in a slight increase in the error rates.

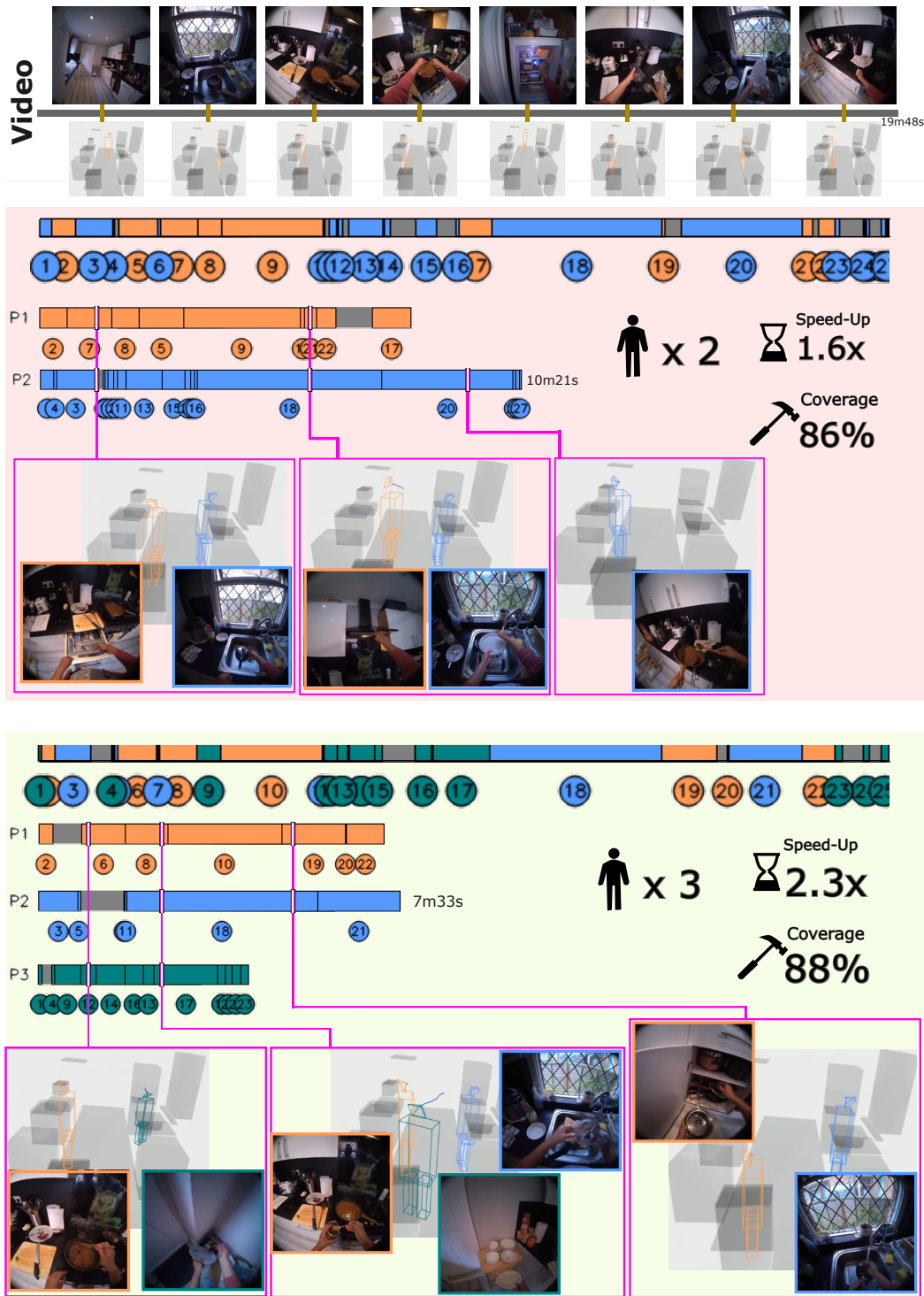


Figure 5. **See also Video Supp: Top.** Our input is single-person egocentric video. The camera wearer (shown also in orange in 3D) performs a combination of cooking, washing up and ordering. **Middle.** 2-Body Parallel execution. Our method achieves a 1.6x speed-up (from 19.8min to 10.4min) with 86% coverage. We show coloured segments (orange/blue) along with 3D representation of where the 2-agents are and their camera views (colour-bordered keyframes). P1 is mostly left to do the cooking, while P2 is washing up and ordering. **Bottom.** 3-Body parallel execution achieving further 2.3x speed-up to 7.5min. P2 is washing up while P3 is drying and storing things away.

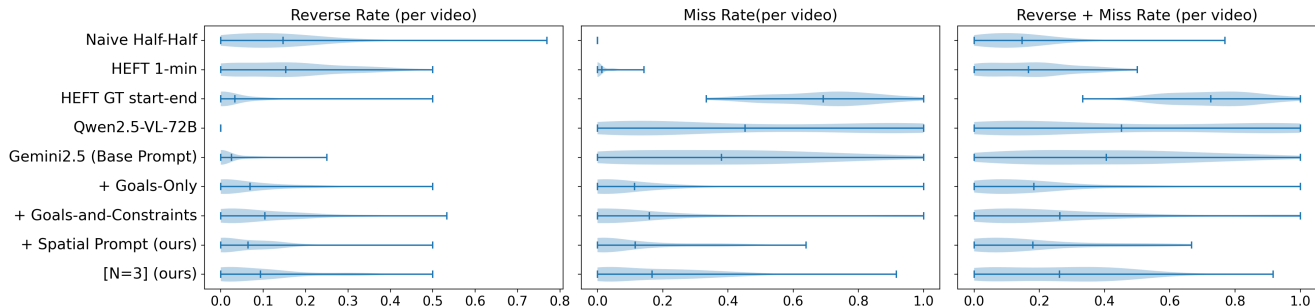


Figure 6. Recipe order distribution over methods.

Method	Coverage (%) \uparrow	Action Coverage (%) \uparrow	Speed-Up \uparrow	Collision Rate (%) \downarrow	Avg. Jump (m) \downarrow	OCR (%) \downarrow	CVR (%) \downarrow
+Goals-and-Constraints	87.4	88.1	1.59	17.5	0.47	0.93	26.3
Raw Trajectory	90.6	91.3	1.49	13.9	0.48	1.17	15.7
GMM (5 comps)	91.3	91.4	1.48	10.8	0.57	0.57	20.3
GMM (10 comps)	86.8	87.0	1.44	10.5	0.55	0.89	21.4
40 \times 40cm	88.3	88.8	1.48	11.5	0.48	0.90	19.8
80 \times 80cm	88.7	89.1	1.40	9.9	0.48	0.57	21.2
120 \times 120cm (Ours)	90.7	91.3	1.40	7.7	0.55	0.64	18.0

Table 3. Spatial Prompt variants on HD-EPIC.

Method	Prep-Step Error / 728			Step-Step Error / 204			Total / 932
	Reverse	Miss	Combined	Reverse	Miss	Combined	
Naive Half-Half	76	0	76	59	0	59	135
HEFT 1-min	86	5	91	52	9	61	152
HEFT GT start-end	15	514	529	4	133	137	666
Qwen2.5-VL-72B	0	225	225	0	72	72	297
Gemini2.5 (Base Prompt)	12	291	303	10	116	126	429
+ Goal-Only	32	73	105	35	32	67	172
+ Goals-and-Constraints	40	111	151	41	61	102	253
+ Spatial Prompt (ours)	27	97	124	27	37	64	188
3-Body Problem (ours)	45	127	172	43	56	99	271

Table 4. Detailed error breakdown on all 60 videos. Columns are grouped into Prep-Step and Step-Step error types, followed by the overall combined count. *Qwen2.5-VL-72B only produces results for 37 out of these 60 videos.

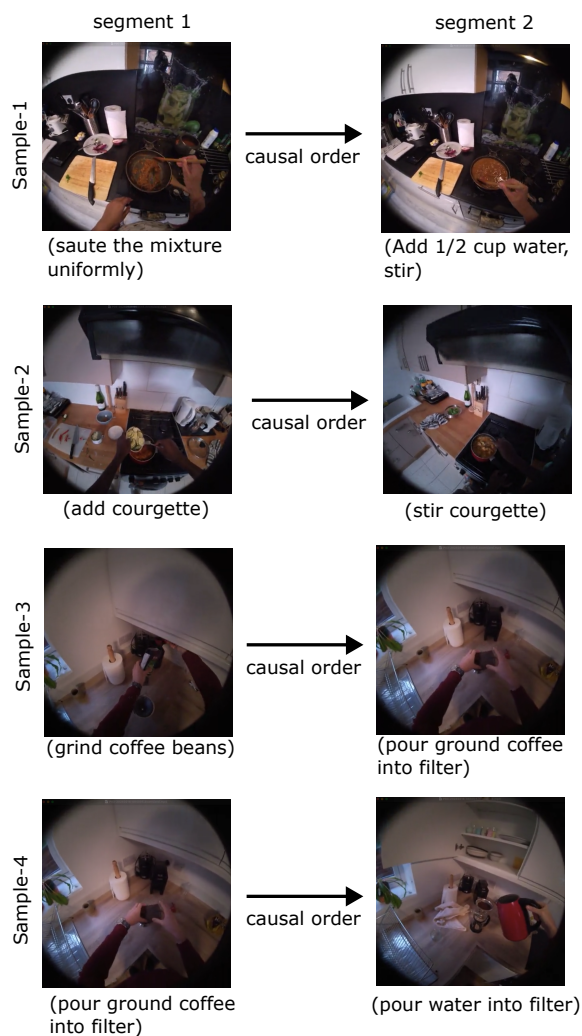


Figure 7. Step-step causal dependency annotation samples. We show one frame in each step segment. We include text to explain the frame; these text snippets can be found in the full recipe annotation of the HD-EPIC dataset.

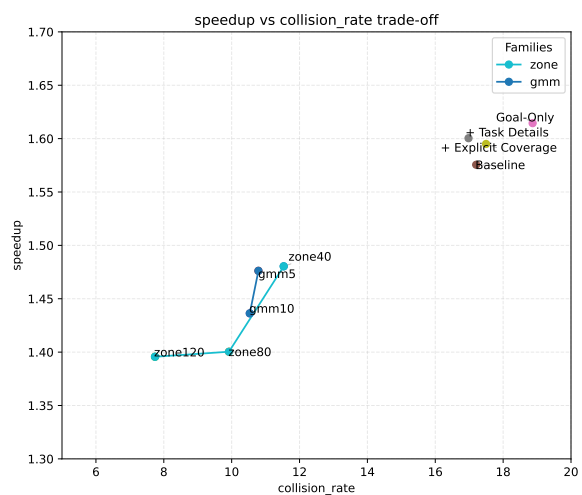


Figure 8. Speed-Up and Collision trade-off of different methods on the HD-EPIC dataset.

D. The Complete Prompt

```
1 # Task Overview
2
3 You are a job planner for a two-agent system.
4 You watch an egocentric video.
5 There are opportunities to parallelise the video to be performed by two agents (P1 and P2)
  efficiently.
6 You need to find such opportunities and make a parallel execution out of the original video,
  while respecting all dependencies and avoiding spatial conflicts.
7 The parallel execution shouldn't have dependency disorder (e.g. pour milk before bottle is
  taken out of the fridge) and shouldn't have 3D spatial conflict (e.g. both accessing the
  fridge).
8 Tell me how to rearrange the clips from the original video into two streams, so that the
  video can be performed by two people jointly.
9
10 # Avoiding Spatial Conflict
11
12 The trajectory CSV file lists the segments where the original person stays in different
  zones: "Z1", "Z2", "Z3", etc.
13 If two tasks from the original video could semantically be done in parallel, but the CSV
  file shows they both occur in the same zone "Z_n", you *must* serialise them.
14 Schedule P1 to work only in "Z_i" durations and P2 to work only in "Z_j" zone such that Z_i
  != Z_j.
15 The spatial reasoning should rely on the trajectory csv exclusively, do not use any knowledge
  from the video.
16 While splitting agents in different zones, remember to still respect the semantics of the
  task execution.
17
18 # Avoiding Semantic Dependency Disorder
19
20 Below are more examples of semantic dependency disorder:
21 1. When making coffee, pour hot water into the coffee before the coffee powder has been
  added to the mug.
22 2. Wash mixer's head while the other agent is still using the mixer.
23 3. Uses the same trash bin at the same time.
24
25 # Covering every moment in the original video
26
27 Note that although this task aims to speed up the video, it should not skip any part of the
  original video. Every second of the original video needs to be covered, ensuring
  coverage = 100%.
28
29 # Format
30
31 Output json format:
32 With two keys "P1" and "P2", each contains a list of jobs (dictionaries).
33 A job is a part of the original video performed by P1 or P2.
34 A job is a dictionary with fields:
35 "new_start": the new start time performed by this person, "start" and "end" are the old
  start/end time in the original video. "text" is the summary text describing the clip of
  the job.
36 Example:
37 ```
38 {
39     "P1": [
40         {
41             "new_start": "00:00",
```

```

42     "start": "00:00",
43     "end": "00:26",
44     "text": "walk in and take from fridge",
45 },
46 {
47     "new_start": "00:26",
48     "start": "00:51",
49     "end": "01:14",
50     "text": "use and put milk into fridge"
51 },
52 {
53     "new_start": "00:49",
54     "start": "01:22",
55     "end": "1:59",
56     "text": "take cereal and mix"
57 }
58 ],
59 "P2": [
60     {
61         "new_start": "00:00",
62         "start": "00:26",
63         "end": "00:44",
64         "text": "put cloth and move bottles",
65     },
66     {
67         "new_start": "00:19",
68         "start": "00:44",
69         "end": "00:51",
70         "text": "take out cup and put onto the table",
71     },
72     {
73         "new_start": "00:26",
74         "start": "01:14",
75         "end": "01:22",
76         "text": "prepare spoon",
77     }
78 ]
79 }
80 ```
81
82 # Fall-back to single-thread
83
84 When it is really hard to schedule more than one agent in a constrained spatial space, a
85 safer solution with single agent is preferred than a dangerous parallel plan with high
86 potential spatial collision.
87
88 # Requirement Summary
89
90 Main requirement: Coverage. To avoid missing any segments of the full video (coverage <
91 100%),
92 keep in mind that every segment in the new parallel plan corresponds to a segment in the
93 original video, and the original segments add up should always cover 100% of the
94 original duration.
95
96 Supplementary requirements:
97 1. Pay attention to Spatial Conflicts. For example, no simultaneous access to the fridge. A
98 better planning may use the same countertop at different times.
99 2. Pay attention to the Object dependency, e.g. place mug before pouring milk.

```